Shape-Dependent Thermal Switching Behavior of Superparamagnetic Nanoislands

M. Bode,* O. Pietzsch, A. Kubetzka, and R. Wiesendanger

Institute of Applied Physics and Microstructure Research Center, University of Hamburg, Jungiusstrasse 11, 20355 Hamburg, Germany

(Received 3 September 2003; published 12 February 2004)

The thermal switching behavior of individual perpendicularly magnetized nanoscale Fe islands consisting of 200–600 atoms only is studied by low-temperature spin-polarized scanning tunneling microscopy. Our results reveal that the switching rate is strongly affected by the particle shape; i.e., elongated islands switch much more rapidly than compact islands of the same volume. This observation is explained by different processes of magnetization reversal. Our results suggest that compact magnetic particles are an ideal choice for future perpendicular magnetic recording media because they are robust against thermal magnetization reversal.

DOI: 10.1103/PhysRevLett.92.067201 PACS numbers: 75.20.–g, 68.37.Ef, 75.75.+a

With the vast growth of the storage density in magnetic media within the past decades we have witnessed a stunning miniaturization of magnetic grains; the so-called "superparamagnetic limit" is rapidly approached [1]. This term describes the critical size below which small magnetic particles may continually reverse their magnetization direction due to thermal agitation. In early theoretical approaches Néel [2] and Brown [3] calculated the switching probability under the assumption of coherent rotation, i.e., at any time — even during the reversal — the magnetic moments of the entire particle remain magnetized in the same direction, behaving like a single giant spin (superparamagnet). Under these requirements the switching rate is described by the so-called Néel-Brown law

$$\nu = \nu_0 \exp\left(-\frac{E_B}{k_B T}\right), \tag{1}$$

with ν_0 the attempt frequency, E_B the energy barrier that separates two degenerate magnetization states (up and down), the Boltzmann constant k_B, and the temperature T. Because of sensitivity limitations, early experiments had to be performed on ensembles of supposably identical particles, and effects related to details of the size and the shape of individual particles were concealed by the averaging process. Only recently it became possible to detect the switching behavior of single particles and to relate it to the particle's geometry as measured in a separate scanning electron or magnetic force microscopy investigation [4–8]. Results obtained on single ferromagnetic, ellipsoidal cobalt particles with a diameter of 25 ± 5 nm are in agreement [7], while measurements performed on elongated particles are in disagreement with the Néel-Brown law [6]. Instead, the latter results indicate that the reversal starts in a small fraction of the particle volume. After nucleation of a reversed domain the associated domain walls propagate through the sample [6].

The shape dependence of the thermally activated magnetization reversal rate has been explored theoretically by Braun [9–11]. For simple sample geometries Braun found an analytical solution which was recently confirmed by Monte Carlo simulations [12]. The relevant parameter which allows one to predict the reversal mechanism is the critical length l_{crit}. In the case of a sufficiently narrow cylinder-shaped particle l_{crit} is given by $2\pi L$, where L is the magnetic exchange length being defined as $L = \sqrt{A/k_{eff}}$ with the exchange stiffness A and the effective anisotropy constant k_{eff}. It was found that short particles of length $l \leq l_{crit}/2$ exclusively reverse their magnetization by coherent rotation. The barrier of this process is the anisotropy energy $E_a = k_{eff} V$ which is proportional to the particle volume V. The resulting switching rate is consistent with Eq. (1). For $l \geq l_{crit}/2$ the nucleation of a reversed domain at one particle end has to be considered. The energy barrier of this process depends on the energy required to create a single 180° domain wall which then propagates from one particle end to the other, given by $E_w = 4a\sqrt{k_{eff} A}$ with a being the wall area. Only for $l > l_{crit}$ the nucleation of a reversed domain in the interior of the sample becomes possible. Braun predicted [9–11] that the energy barrier related to domain wall creation in an elongated particle with $l \geq l_{crit}/2$ is lower than the barrier for coherent rotation of a compact particle of the same volume, leading to a crossover between the two reversal mechanisms around $l_{crit}/2$. Thus the switching rate should depend on the particle shape.

Although a detailed knowledge of the critical length l_{crit} is highly desirable for the future development of ultrahigh-density magnetic recording, Braun's prediction could not yet be verified. We have used the high spatial and magnetic sensitivity of spin-polarized scanning tunneling microscopy (SP-STM) to directly correlate the shape and size of Fe particles with the individually measured switching rates. Indeed, our results reveal that the superparamagnetic limit of out-of-plane magnetized particles is strongly shape dependent, i.e., oblong particles switch much more often than compact, almost circular particles of equal volume. Our results suggest that compact magnetic particles are an ideal choice for future

magnetic recording media because they are robust against thermal magnetization reversal.

The measurements were performed with a scanning tunneling microscope designed for high-resolution studies of surface magnetism [13] at temperatures between $12\ \mathrm{K} \leq T \leq 27\ \mathrm{K}$. In order to exclude any unwanted dipolar tip-sample interaction we used antiferromagnetic Cr coated tips which were sensitive to the out-of-plane component of the sample magnetization [14]. Details of the contrast mechanism of SP-STM are described elsewhere [15]. Nanoscale magnetic Fe islands of monolayer (ML) thickness were prepared under ultrahigh vacuum conditions ($p \leq 1 \times 10^{-10}$ mbar) on Mo(110) at room temperature. The growth mode can be modified by optional subsequent thermal annealing which results in step-flow growth leading to quasi-infinite nanowires of single atomic height.

Figure 1(a) shows a constant-current STM image of the topography of 0.25 ML Fe deposited on Mo(110) at room temperature. Two atomically flat Mo(110) terraces are visible. They are decorated with Fe islands which are slightly elongated along the [001] direction [16,17]. Simultaneously with the topography we have recorded maps of the differential conductance dI/dU using an out-of-plane sensitive Cr coated probe tip [Fig. 1(b)]. Although the spin-averaged electronic properties of all Fe islands are identical (not shown here) one can recognize bright and dark islands in Fig. 1(b) representing two different values of the local dI/dU signal. This variation is caused by spin-polarized vacuum tunneling between the magnetic tip and islands which are magnetized perpendicularly either up or down.

Most of the islands exhibit a surface area $a \geq 40\ \mathrm{nm}^2$ and therefore possess a barrier large enough to inhibit superparamagnetic switching at $T = 13\ \mathrm{K}$. Consequently, their magnetization direction remains constant resulting in the same dI/dU signal in successive scans. Few smaller islands, however, are found to be magnetically unstable on the time scale of the experiment, i.e., several minutes. Such an island with $a = 26 \pm 1\ \mathrm{nm}^2$ is shown at higher magnification in the inset of Fig. 1(b). The dI/dU signal changes between two subsequent scan lines from a low value (dark) at an early time of the scan (bottom part of the image) to a higher value (bright). This signal variation is caused by superparamagnetic switching [18].

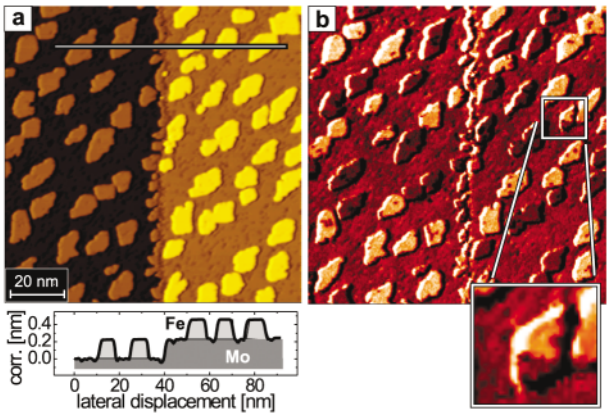

FIG. 1 (color). (a) Topographic STM image and (b) the simultaneously measured out-of-plane sensitive magnetic dI/dU signal of two Mo(110) terraces decorated with Fe islands (overall coverage 0.25 ML). The line section (lower panel) reveals that the substrate's step edge and the islands are of monatomic height (≈ 2 Å). During image recording one island switches from dark to bright (inset). Measurement parameters are $T = 13\ \mathrm{K}$, $U = 90\ \mathrm{mV}$, and $I = 1\ \mathrm{nA}$.

From Eq. (1) it is expected that the switching rate ν exponentially increases with increasing temperature. We checked this by successively scanning along the same line thereby periodically visiting four islands "a"–"d"(inset of Fig. 2). Measurements were performed at temperatures $T_1 = 13\ \mathrm{K}$ and $T_2 = 19\ \mathrm{K}$ for 5.5 min with a line repetition frequency of 3 Hz. At every passage the dI/dU signal of the islands was recorded (Fig. 2). At $T_1 = 13\ \mathrm{K}$ (left panel) the relatively large islands a ($a = 30.0\ \mathrm{nm}^2$), d ($a = 71.2\ \mathrm{nm}^2$), and c ($a = 28.2\ \mathrm{nm}^2$) do not switch. This magnetic stability is a result of their large anisotropy energy that prevents superparamagnetic switching at this temperature. In contrast, island b ($a = 17.8\ \mathrm{nm}^2$) with its lower barrier reverses its magnetization direction 31 times within the observation time. In qualitative agreement with Eq. (1) the switching rate of any island increases as the temperature is increased to $T_2 = 19\ \mathrm{K}$ (right panel). Islands a, c, and d reverse their magnetization direction 18, 10, and 1 times, respectively. Since the switching rate of island b exceeds the line repetition rate, we cannot resolve single switching events and an intermediate and blurred dI/dU signal is measured above b.

The effective anisotropy constant of individual superparamagnetic particles can be determined by temperature-dependent measurements of the switching rate. Transformation of the Néel-Brown law gives

$$k_{\mathrm{eff}} = \ln\frac{\nu_1}{\nu_2}\frac{k_{\mathrm{B}}}{V}\left(\frac{1}{T_2} - \frac{1}{T_1}\right)^{-1}, \qquad (2)$$

where $\nu_{1,2}$ denote switching rates measured at $T_{1,2}$. We observed two islands with a nonzero and finite switching rate at two temperatures $T_1 = 19\ \mathrm{K}$ and $T_2 = 26\ \mathrm{K}$: the first one has an area of $28.8\ \mathrm{nm}^2$ and switching rates of $\nu_1 = (4.0 \pm 2.0) \times 10^{-4}\ \mathrm{s}^{-1}$ and $\nu_2 = 0.37 \pm 0.11\ \mathrm{s}^{-1}$, while the second island with an area of $33.3\ \mathrm{nm}^2$ switched at rates $\nu_1 = (3.0 \pm 1.7) \times 10^{-4}\ \mathrm{s}^{-1}$ and $\nu_2 = 0.33 \pm 0.1\ \mathrm{s}^{-1}$. Insertion into Eq. (2) results in $k_{\mathrm{eff}} = 1.16^{+0.17}_{-0.13} \times 10^6\ \mathrm{J/m}^3$ and $k_{\mathrm{eff}} = 1.04^{+0.16}_{-0.45} \times 10^6\ \mathrm{J/m}^3$ for the two islands, respectively. In the following we assume an effective anisotropy $k_{\mathrm{eff}} = 1.10^{+0.12}_{-0.24} \times 10^6\ \mathrm{J/m}^3$.

Figure 3 shows (a) the topography and (b) a map of the magnetic dI/dU signal of 23 numbered islands prepared by room-temperature deposition of 0.08 ± 0.01 ML Fe/Mo(110). Except for islands "19" and "23" the interparticle distance is sufficiently large to exclude any significant dipolar interaction. The complete series consists of

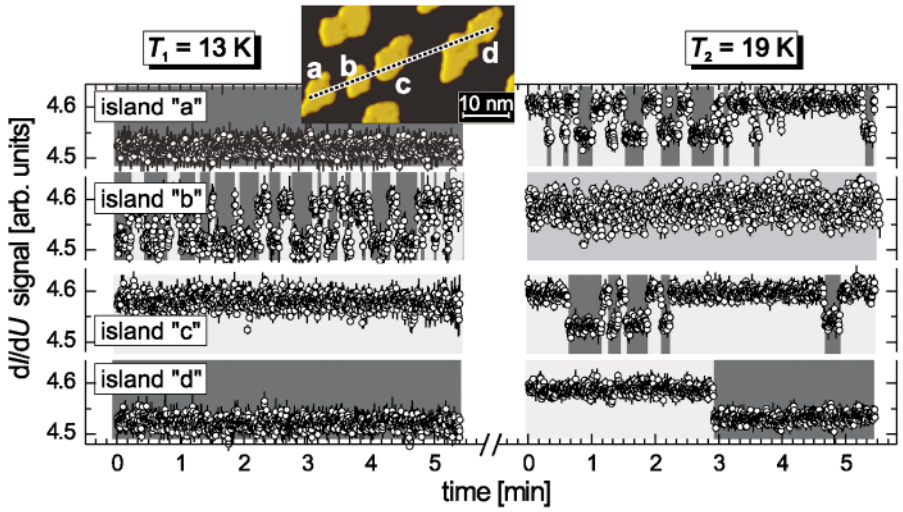

FIG. 2 (color). Magnetic switching behavior of the Fe islands a–d (inset) measured at $T = 13 \pm 1$ K (left panel) and $T = 19 \pm 1$ K (right panel). The switching rate increases with increasing temperature thereby proving the thermal nature of the observed effect. At $T = 19 \pm 1$ K the switching rate of island b exceeds the line repetition rate resulting in an intermediate and blurred signal.

53 images measured over a total time of more than 5 h. By making use of the three different sampling rates of our experiment, i.e., the increment between successive pixels (≈ 1 ms), successive scan lines (≈ 1 s), and between successive images (≈ 5 min), we are able to follow the magnetization reversal behavior of individual islands over a wide frequency range. The switching rates are plotted semilogarithmically versus the island area in Fig. 3(c). Each data point is labeled with the related island number assigned in Fig. 3(a). Although the general trend — small islands switch more often than large islands — can clearly be recognized, the data points scatter strongly around the expected linear relation. For example, albeit the area of the islands marked green ("11," "18," and "27") is smaller than the area of the islands marked red ("3," "16," and "25"), the switching rates of the former are 1 to 2 orders of magnitude smaller. The topographic images in the insets of Fig. 3(c) reveal that this contraintuitive behavior is associated with the island shape: while the red (rapidly switching) islands are elongated the green (slowly switching) islands are much more compact.

According to Braun's theory the particular magnetization reversal mechanism of individual islands depends on the ratio between the lateral particle dimensions and the magnetic exchange length L. By making use of the fact that L is also linked to the domain wall width w by $w = 2L = 2(A/k_{\mathrm{eff}})^{1/2}$, we are able to determine L independently [19] by measuring domain wall profiles. While we cannot observe domain walls in small islands due to their fast dynamics, static walls can be found in monatomic Fe nanowires grown at the step edges of the Mo(110) substrate (Fig. 4). Similar to Fe double-layer nanowires on W(110) [20,21], the magnetic domain structure of nanowires on Mo is governed by an antiparallel orientation of adjacent nanowires due to dipolar interaction [21]. At structural imperfections occasionally domain walls can be found. The overview of Fig. 4(a) shows the topography (left panel) and the magnetic dI/dU signal (middle panel) of six nanowires. In four nanowires a domain wall can be recognized. We have zoomed into one domain wall [Fig. 4(b)]. From a micromagnetic fit to the measured wall profile [19] we obtain $w = 2.9 \pm 0.1$ nm, thus $L = 1.45 \pm 0.05$ nm [22]. Using k_{eff} as determined above we find $A = 2.3^{+0.5}_{-0.7} \times 10^{-12}$ J/m.

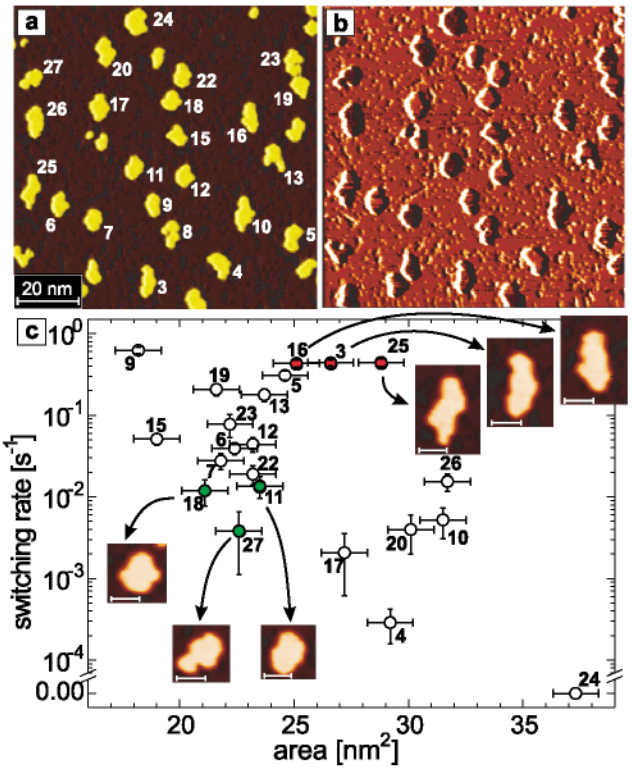

FIG. 3 (color). (a) Topography and (b) magnetic dI/dU signal of numbered Fe islands on Mo(110). (c) Plot of the switching rate versus the area of individual islands. The scatter of the switching rate points to a shape-dependent crossover from coherent rotation of compact Fe islands towards nucleation and expansion of reversed domains in elongated islands. Insets: topography of selected Fe islands (scale bar: 5 nm).

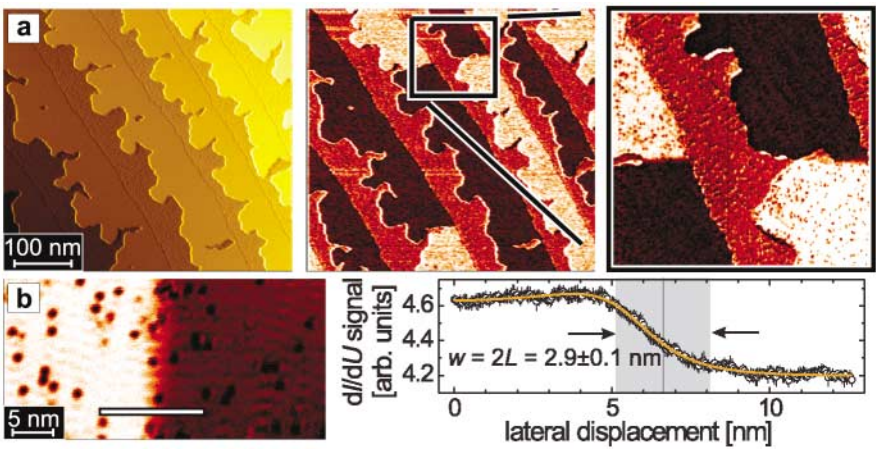

FIG. 4 (color). (a) Overview showing the topography (left panel) and magnetic dI/dU signal (middle panel) of Fe nanowires on Mo(110). Four domain walls can be recognized. Right panel: two domain walls at higher magnetification. (b) Zoom into the domain wall region (inset, rotated by 90°). The domain wall width is $w = 2.9 \pm 0.1$ nm (orange line).

Once L is known we can determine the critical particle length of Fe monolayer islands on Mo(110) to $l_{\mathrm{crit}} = 2\pi L = 9.1 \pm 0.3$ nm. Comparing this value with the typical diameter $d \approx 5$ nm of the compact islands marked green in Fig. 3(c), we find that d is almost equal to $l_{\mathrm{crit}}/2$. Therefore, we identify coherent rotation as the dominating mechanism of magnetization reversal in the compact particles 11, 18, and 27. Since we know the switching rate of, e.g., particle 11, $\nu_{11} = 0.013 \pm 0.004\ \mathrm{s}^{-1}$ and its volume $V_{11} = (4.7 \pm 0.2) \times 10^{-27}\ \mathrm{m}^3$ we may — using the magnetic material parameters k_{eff} and A as found above — determine the attempt frequency of that particle to $\nu_0 = 4.08^{+0.14}_{-3.24} \times 10^{10}\ \mathrm{s}^{-1}$ [23] and the energy barrier against coherent rotation which amounts to $E_{\mathrm{B}} = 5.17^{+0.85}_{-1.37} \times 10^{-21}$ J.

Island 16 exhibits approximately the same area as island 11. Nevertheless, its switching rate is 31 times higher. This difference is due to a different process of magnetization reversal. The elongated shape of island 16 (length $l = 8.65 \pm 0.4$ nm $\approx l_{\mathrm{crit}}$) leads to the fact that the energy of a domain wall E_{w} along the short axis of the island is lower than the barrier against coherent rotation [9–11]. The cross-sectional area of island 16 is $0.6 \pm 0.1\ \mathrm{nm}^2$. With this value we may estimate $E_{\mathrm{w}} = 3.81^{+1.37}_{-1.46} \times 10^{-21}$ J, i.e., for elongated islands the trend is $E_{\mathrm{w}} < E_{\mathrm{B}}$, albeit within a large error margin. This explains qualitatively the higher switching rate compared to that of compact islands of equal volume.

In summary, we have studied the shape dependence of thermal magnetization reversal of individual perpendicularly magnetized Fe nanoislands on Mo(110). Our results show that — comparing islands of equal volume — the switching rates of elongated islands are much higher than that of compact islands. This result is explained in the spirit of Braun's model by different paths of magnetization reversal, i.e., coherent switching of compact islands and domain wall formation for elongated islands.

We thank H.-B. Braun, U. Nowak, and J. Kötzler for enlightening discussions. Financial support from the DFG (Grant No. Wi 1277/19-1) and Graduiertenkolleg "Physik nanostrukturierter Festkörper" is acknowledged.

*Corresponding author.
Electronic addresses: mbode@physnet.uni-hamburg.de
http://www.nanoscience.de/bode

[1] D. Weller and A. Moser, IEEE Trans. Magn. **35**, 4423 (1999).
[2] M. L. Néel, Ann. Geophys. **5**, 99 (1949).
[3] W. F. Brown, Phys. Rev. **130**, 1677 (1963).
[4] M. Lederman, G. A. Gibson, and S. Schultz, J. Appl. Phys. **73**, 6961 (1993).
[5] M. Lederman, S. Schultz, and M. Ozaki, Phys. Rev. Lett. **73**, 1986 (1994).
[6] W. Wernsdorfer *et al.*, Phys. Rev. Lett. **77**, 1873 (1996).
[7] W. Wernsdorfer *et al.*, Phys. Rev. Lett. **78**, 1791 (1997).
[8] W. Wernsdorfer *et al.*, Phys. Rev. B **55**, 11 552 (1997).
[9] H.-B. Braun, Phys. Rev. Lett. **71**, 3557 (1993).
[10] H.-B. Braun, Phys. Rev. B **50**, 16 501 (1994).
[11] H.-B. Braun, J. Appl. Phys. **85**, 6172 (1999).
[12] D. Hinzke and U. Nowak, Phys. Rev. B **61**, 6734 (2000).
[13] O. Pietzsch *et al.*, Rev. Sci. Instrum. **71**, 424 (2000).
[14] A. Kubetzka *et al.*, Phys. Rev. Lett. **88**, 057201 (2002).
[15] M. Bode, Rep. Prog. Phys. **66**, 523 (2003).
[16] M. Tikhov and E. Bauer, Surf. Sci. **232**, 73 (1990).
[17] J. Malzbender *et al.*, Surf. Sci. **414**, 187 (1998).
[18] We emphasize that the image in the inset does not represent a snapshot of the switching island *during* the magnetization reversal. This process occurs on a time scale ($\approx 10^{-12}$ s) being much shorter than even the time increment between subsequent pixels ($\approx 10^{-3}$ s). Instead, the contrast is caused by the fact that the imaging of the island accidentally coincided with the moment of its magnetization reversal.
[19] A. Hubert and R. Schäfer, *Magnetic Domains* (Springer, Berlin, 1998).
[20] O. Pietzsch *et al.*, Phys. Rev. Lett. **84**, 5212 (2000).
[21] H. J. Elmers, J. Hauschild, and U. Gradmann, Phys. Rev. B **59**, 3688 (1999).
[22] Within the error margin the wall width w does not depend on the position of the section.
[23] Since the calculation of the attempt frequency employs several parameters with relatively large error bars, the values obtained for different compact islands strongly scatter between 2×10^{-8} and $5 \times 10^{11}\ \mathrm{s}^{-1}$.